A Consensus Equilibrium Approach for 3D Land Seismic Shots Recovery

Paul Goyes-Peñafiel, Edwin Vargas, *Student Member, IEEE,* Claudia V. Correa, *Member, IEEE,* William Agudelo, Brendt Wohlberg, *Senior Member, IEEE,* and Henry Arguello *Senior Member, IEEE*

***Abstract*—Physical and budget constraints often result in inadequate sampling for accurate subsurface imaging. Pre-processing approaches, such as missing trace interpolation, are typically employed to enhance seismic data in such cases. The compressed sensing (CS) framework has been applied for modeling missing seismic data, which is estimated by sparsity-based computational algorithms. While existing work mainly focuses on recovering missing traces resulting from receiver subsampling, source subsampling has greater economical advantages, as sources are more expensive than receivers. Moreover, stronger image models different from sparsity have not been explored for source recovery. This work presents a consensus equilibrium (CE) approach to recover missing seismic shots, which enables to incorporate various regularization operators modeling different data priors. Simulation results from a real 3D land seismic data set demonstrate that the CE approach provides more accurate estimations of the linear and hyperbolic events in the recovered shots, compared with pure sparsity-based reconstructions.**

***Index Terms*—Seismic Shot recovery, Consensus Equilibrium, Regularization.**

I. Introduction

SOURCE sampling plays an essential role in seismic acquisition due to its direct effect on the quality and resolution of the seismic imaging process. Research efforts have focused on survey design to obtain high density sampling, as well as new techniques for the improvement of data acquired in complex areas including topographical, environmental, and social restrictions. Missing trace recovery, which involves interpolation techniques [1]–[5], is one of the major approaches to address the aforementioned quality issues.

In contrast to high density sampling, the compressed sensing (CS) framework establishes that a signal can be accurately recovered from far fewer samples than those dictated by the classical Shannon-Nyquist theory, given that the signal is compressible in a particular domain, i.e. it has an approximate sparse representation [6], [7]. Based on this premise, CS has been recently introduced to the seismic data acquisition process [8]–[12]. In particular, it has favored the design of subsampling approaches that result in less-expensive field acquisitions [13], as it allows the designer to reduce the number of receivers, such that less data is captured. The reduced number of receivers translates to missing traces, which can be recovered by exploiting the compressible nature of the signal in a given transformation basis [14] even for irregularly sampled traces [15], or deep learning approaches [5], [16], [17]. An obvious choice of a dictionary for seismic data is provided by the curvelet transform, which is a type of directional anisotropic wavelet that can effectively capture textural characteristics of these data [18]. Other common transformations employed for seismic signal compression include Seislet, and atom waves [19]–[24]. One of the main drawbacks of receiver-subsampling approaches is that CS capabilities are not fully exploited as the cost of a receiver is considerably less than that of a source. Moreover, missing seismic sources are related to typical environmental, topographic or social constraints, where data acquisition is prohibited. Nevertheless, subsampling of the seismic sources has not received much attention in the literature. For instance, methods to recover wavefields from missing sources in 3D othogonal geometries, exploiting local and non-local data redundancies were developed in [25], [26].

In general, the selection of the dictionary is critical for the effectiveness of sparsity-based methods, and it is not a trivial problem for seismic data. Transform basis such as Curvelets and Seislets, might not be able to appropriately represent particular signal features that vary among geographical locations [20], and they cannot be adaptively selected according to the data characteristics [20], [27]. Therefore, this work proposes to use alternative regularization operators, such as plug and play priors (PnP), to complement sparsity-based fidelity terms in the seismic source CS reconstruction problem. In particular, PnP enables the embedding of state-of-the-art denoising algorithms as priors in the reconstruction process [28]. Essentially, the proposed approach takes advantage of the intrinsic capabilities of the consensus equilibrium (CE) [29] optimization framework (CE) to deal with multiple regularization functions, i.e. sparsity along with various denoising operators, such that the missing seismic source data can be accurately recovered. Simulations on a real 3D seismic data set verify the quality performance of the proposed method. Specifically, the CE approach provides more accurate estimates of the linear and hyperbolic events in the recovered shots. Further, it leads to precise noise and data cut-off frequencies when compared to purely sparsity or plug and play denoising-based methods.

II. Subsampled Seismic Data Acquisition Model

Seismic data can be viewed as three-dimensional structures representing L samples in time of the reflected energy emitted

P. Goyes-Peñafiel, C. V. Correa and H. Arguello are with the Department of Computer Science, Universidad Industrial de Santander, Bucaramanga, Colombia, 680002.

E. Vargas is with the Department of Electronics Engineering, Universidad Industrial de Santander, Bucaramanga, Colombia, 680002.

W. Agudelo is with the Colombian Petroleum Institute-ECOPETROL, Piedecuesta, Colombia, 681011.

B. Wohlberg is with Theoretical Division, Los Alamos National Laboratory, Los Alamos, NM 87545 USA.

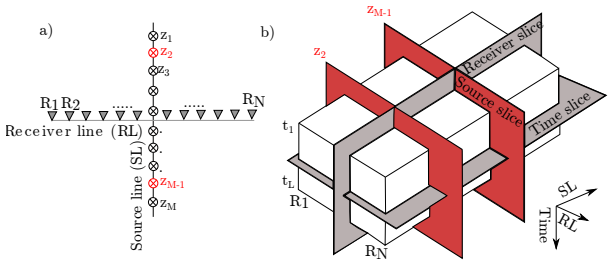

Fig. 1. (a) Full cross-spread acquisition and (b) Subsampled cross-spread by removing the seismic sources at z_2 and z_{M-1}

by M sources, captured by N receivers, as illustrated in Figure 1(a). In particular, this cross-spread configuration consists of a source line orthogonally intercepted by a receiver line, resulting in a subset of the general 3D seismic acquisition. This is one of the most common configurations because it allows the receiver line to conveniently register the seismic structures and provides seismic signals with less coherent noise, e.g. ground roll [25].

Letting $\mathbf{x} \in \mathbb{R}^{MNL}$ be the vector representation of the full seismic cube $\mathbf{X}$, illustrated in Fig. 1(b), the acquisition process can be modeled as a system of linear equations given by

$$\mathbf{y} = \mathbf{\Phi}\mathbf{x} + \boldsymbol{\omega}, \tag{1}$$

with $\mathbf{\Phi} \in \mathbb{R}^{MN(L-k)\times MNL}$ modeling the acquisition operator defined as $\mathbf{\Phi} = \mathbf{S} \otimes \mathbf{I}_{MN}$, where $\otimes$ represents the Kronecker product, $\mathbf{I}_{MN}$ is a $MN \times MN$ identity matrix, $\mathbf{S} \in \mathbb{R}^{L-k\times L}$ is an identity matrix, whose k rows corresponding to the linear indices of the missing sources have been set to zero, such that it models the source subsampling effect, and $\boldsymbol{\omega}$ accounts for the acquisition noise. The acquired seismic shots $\mathbf{y}$ are then used to estimate the whole data set including k missing shots. The traditional inverse CS problem exploits the sparsity data prior on a given dictionary $\mathbf{D} \in \mathbb{R}^{MNL\times MNL}$ such as Wavelets or Curvelets [14]. Thus, the recovered data is the solution to the problem

$$\arg\min_{\mathbf{x}} (1/2)||\mathbf{y} - \mathbf{\Phi}\mathbf{x}||_2^2 + ||\mathbf{D}\mathbf{x}||_1 \ . \tag{2}$$

Even though this sparsity formulation has been successful for seismic data recovery, it might not accurately model complex structures inherent to these data since the ℓ_1 norm is a coarse prior. Thus, to the best of the authors' knowledge, stronger image models have not been to date explored for recovering missing seismic shots. The following section presents an implicit prior defined by the image model in denoising algorithms, which will be jointly used with a sparsity prior in the reconstruction process.

III. Consensus Equilibrium Approach for Source Reconstruction

In recent years, the plug and play priors (PnP) method has become popular as an alternative mechanism for incorporating image denoisers as priors within more general inverse problems [28]. This framework has the advantage of enabling the embedding of state-of-the-art denoising algorithms in the reconstruction process even if the denoiser cannot be expressed as an optimization problem. We propose to leverage the advantages of the implicit image model in a denoiser such as BM3D [30] as an alternative to the sparsity model, or as a complement to it, for the recovery of seismic sources. Since our data is three-dimensional, a volumetric denoiser such as the BM4D [31] would seem to be a natural choice, but the computation resources required for such volumetric denoisers is too high and could extend the time of recovering the seismic data from hours to days. We therefore propose to apply BM3D through receiver and time slices, as illustrated in Fig. 1 (b), as an efficient mechanism for employing two-dimensional denoisers to three-dimensional data [32].

The recovery of seismic sources using multiple regularization functions can be modeled as the optimization problem

$$\arg\min_{\mathbf{x}} \ f(\mathbf{x}) + \sum_i g_i(\mathbf{x}) \tag{3}$$

where the function f represents the data fidelity term and the functions g_i are different regularization functions.

Since we aim to use multiple regularization terms, we employ the consensus equilibrium (CE) framework, which can be viewed as a generalization of PnP that supports multiple data fitting and regularization terms [29]. To the best of our knowledge, neither the PnP nor the CE framework have been previously applied in the context of a seismic source reconstruction problem.

In the following, we first present the general mathematical formulation of the consensus equilibrium theory within the seismic shot reconstruction problem, and then we present the mathematical formulations of the particular regularization functions employed in our work.

Formally, to solve problem (3) using CE, we first reformulate it as the consensus optimization problem given by

$$\begin{aligned} \underset{\mathbf{x},\mathbf{x}_i}{\text{argmin}} \quad & \sum_i^K h_i(\mathbf{x}_i) \\ \text{subject to} \quad & \mathbf{x}_i = \mathbf{x} \end{aligned} \tag{4}$$

where the functions h_i include both the data fidelity term and the regularization functions (e.g. $h_0 = f$ and $h_i = g_{i+1}$). Each h_i corresponds to a vector-valued *agent* map $H_i : \mathbb{R}^n \to \mathbb{R}^n$, with $i = 1, \cdots, K$. If function h_i is known explicitly, then the corresponding *agent* is its proximal operator

$$H_i(\mathbf{v}) = \underset{\mathbf{x}}{\text{argmin}} \ \left\{ \frac{\|\mathbf{v} - \mathbf{x}\|^2}{2\sigma^2} + h_i(\mathbf{x}) \right\} \ , \tag{5}$$

but the main value of this technique is its ability to employ agents that are not necessarily associated with a function h_i [29].

These agents are in *equilibrium* for $(\mathbf{x}^*, \mathbf{u}^*) \in (\mathbb{R}^n, \mathbb{R}^{Kn})$ such that

$$\begin{aligned} & H_i(\mathbf{x}^* + \mathbf{u}_i^*) = \mathbf{x}^*, \quad i = 1, \cdots, K \\ & \sum_{i=1}^K \mathbf{u}_i^* = 0 \ . \end{aligned} \tag{6}$$

These equations are solved by rewriting them in unconstrained form and expressing the solution in terms of a fixed

point problem. First, for vector $\mathbf{v} \in \mathbb{R}^{Kn}$, define $\mathbf{H}, \mathbf{G}_\mu : \mathbb{R}^{Kn} \to \mathbb{R}^{Kn}$ as

$$\mathbf{H}(\mathbf{v}) = \begin{pmatrix} H_1(\mathbf{v}_1) \\ \vdots \\ H_K(\mathbf{v}_K) \end{pmatrix} \qquad \mathbf{G}_\mu = \begin{pmatrix} \bar{\mathbf{v}}_\mu \\ \vdots \\ \bar{\mathbf{v}}_\mu \end{pmatrix} \tag{7}$$

where $\overline{\mathbf{v}}_\mu$ is the average vector given by $\overline{\mathbf{v}}_\mu = \frac{1}{K}\sum_{i=1}^{K} \mathbf{v}_i$, and define $\hat{\mathbf{x}}$ as denoting K copies of $\mathbf{x} \in \mathbb{R}^n$ stacked vertically.

With this reformulation, the CE equations (6) can be written as

$$\begin{aligned} \mathbf{H}(\hat{\mathbf{x}}^* + \mathbf{u}^*) &= \hat{\mathbf{x}}^* \\ \overline{\mathbf{u}}_\mu^* &= 0 \,. \end{aligned} \tag{8}$$

Following theorem 2 and corollary 3 in [29], the solution of these equations is the point $(\mathbf{x}^*, \mathbf{u}^*)$, if and only if, the point $\mathbf{v}^* = \hat{\mathbf{x}}^* + \mathbf{u}^*$ satisfies $\bar{\mathbf{v}}_\mu = \mathbf{x}^*$ and

$$(2\mathbf{G}_\mu - \mathbf{I})\,(2\mathbf{H} - \mathbf{I})\,\mathbf{v}^* = \mathbf{v}^* \,. \tag{9}$$

This implies that $\mathbf{v}^*$ is a fixed point of the operator $\mathbf{T} = (2\mathbf{G}_\mu - \mathbf{I})\,(2\mathbf{H} - \mathbf{I})$, which can be found via the Mann iterations [29]

$$\mathbf{v}^{\ell+1} = (1-\rho)\mathbf{v}^\ell + \rho\mathbf{T}(\mathbf{v}^\ell) \,, \tag{10}$$

where $\rho \in (0,1)$ is an algorithm parameter. Given the fixed point $\tilde{\mathbf{v}} = [\tilde{\mathbf{v}}_1, \cdots, \tilde{\mathbf{v}}_K]^T$ found via these iterations, the solution to the CE problem, corresponding in this case to the recovered seismic shots, is given by $\tilde{\mathbf{x}} = 1/K \sum_{i=1}^{K} \tilde{\mathbf{v}}_i$.

The agents used in this work to construct $\mathbf{H}$ in (7), required by the operator $\mathbf{T}$ in (10), are defined as

$$H_1(\mathbf{v}_1) = \underset{\mathbf{x}}{\text{argmin}} \left\{ \frac{\|\mathbf{x} - \mathbf{v}_1\|^2}{2\sigma^2} + \|\mathbf{y} - \mathbf{\Phi}\mathbf{x}\| \right\} \tag{11}$$

$$H_2(\mathbf{v}_2) = \underset{\mathbf{x}}{\text{argmin}} \left\{ \frac{\|\mathbf{x} - \mathbf{v}_2\|^2}{2\sigma^2} + \lambda\|\mathbf{D}\mathbf{x}\|_1 \right\} \tag{12}$$

$$H_3(\mathbf{v}_3) = \text{BM3D}_t(\mathbf{v}_3, \sigma_n) \tag{13}$$

$$H_4(\mathbf{v}_4) = \text{BM3D}_r(\mathbf{v}_4, \sigma_n), \tag{14}$$

where BM3D_t and BM3D_r refer to the denoising of the data cube along time and receiver slices, respectively; σ and λ are parameters controlling the strength of the regularization; $\mathbf{D}$ is a dictionary for the sparse representation of the seismic data while the parameter σ_n is the variance parameter employed in the BM3D algorithm. It should be noted that the variance parameter is the same for both denoisers.

IV. Simulations and Results

Simulations were conducted to evaluate the CE approach in the reconstruction of missing shots of a cross-spread. Specifically, we used CE with three regularizers: BM3D through time and receiver slices and sparsity prior in the Wavelet domain, with the proximal mappings in (11). The experiments use the BM3D version from [30], which was implemented through the Python wrapper publicly available at [33]. The results are compared with respect to two methods: (i) sparsity-based regularization using the Symlet-8 Wavelet transform [25]; (ii) reconstruction based on plug and play priors (PnP) [28], where the BM3D denoiser was set as the mapping along receiver slices. A variant of PnP with the sparsity initialization was also considered (PnP-i). The crucial task of tuning the parameters σ and λ for CE was performed via a grid search. The employed parameters are summarized in Table I.

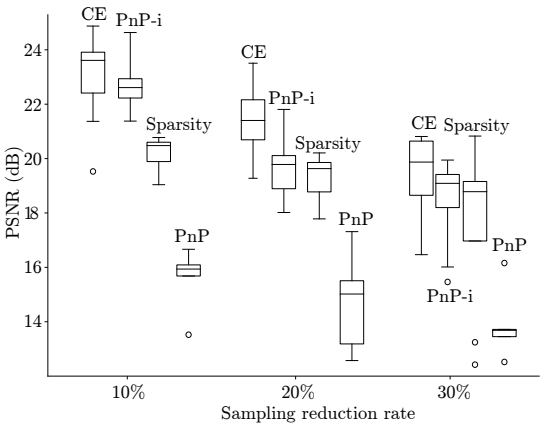

Fig. 2. Average PSNR evaluation as a function of the sampling reduction rate for PnP, Sparsity and CE reconstruction approaches. Sampling reduction rate represents the percentage of removed sources.

TABLE I
Parameter configuration for the different evaluated methods.

Method	σ	λ	σ_n
Sparsity	0.008	0.001	-
PnP	0.0001	-	0.1
PnP-i	0.008	-	0.001
CE	0.008	0.00001	0.001

The experiments employed jittered subsampling to select the subset of shots to be removed. This subsampling method consists in applying a compression rate to blocks of shots, such that the same number of shots is removed for all blocks [34]. The seismic data set employed for the simulations comprises a 3D land swath acquisition project from South Texas, which was rearranged to a cross-spread by using a geometric analysis of the seismic acquisition; the original data set size was 3000 time samples, 120 receivers, and 128 sources. Additional details regarding this data set can be found in [35]. Due to the computational burden of the available equipment, a subset of 1001 time samples, 90 receivers, and 18 sources was used. To assess the accuracy of the reconstructions, we used the peak signal-to-noise ratio (PSNR) value in the frequency-wavenumber domain (FK) exactly as described by [22], and the Structural Similarity Image Metric (SSIM) from [36]. Although the PSNR in the FK domain shows significant changes in the reconstructed seismic signal, it does not take into account the similarity of the seismic events perceived, which is an important aspect to be analyzed in seismic data, we took a special consideration with the SSIM metric, since it is a novel metric for the evaluation of these data. Figure 2 illustrates the attained PSNR for different sampling reduction rates, i.e. the percentage of removed sources, using the approaches under comparison. These results are the average PSNR for all recovered shots on each run trial, and a total of 10 experiment trials, each with a different jittered subsampling realization, were conducted for each case. The PnP approach without

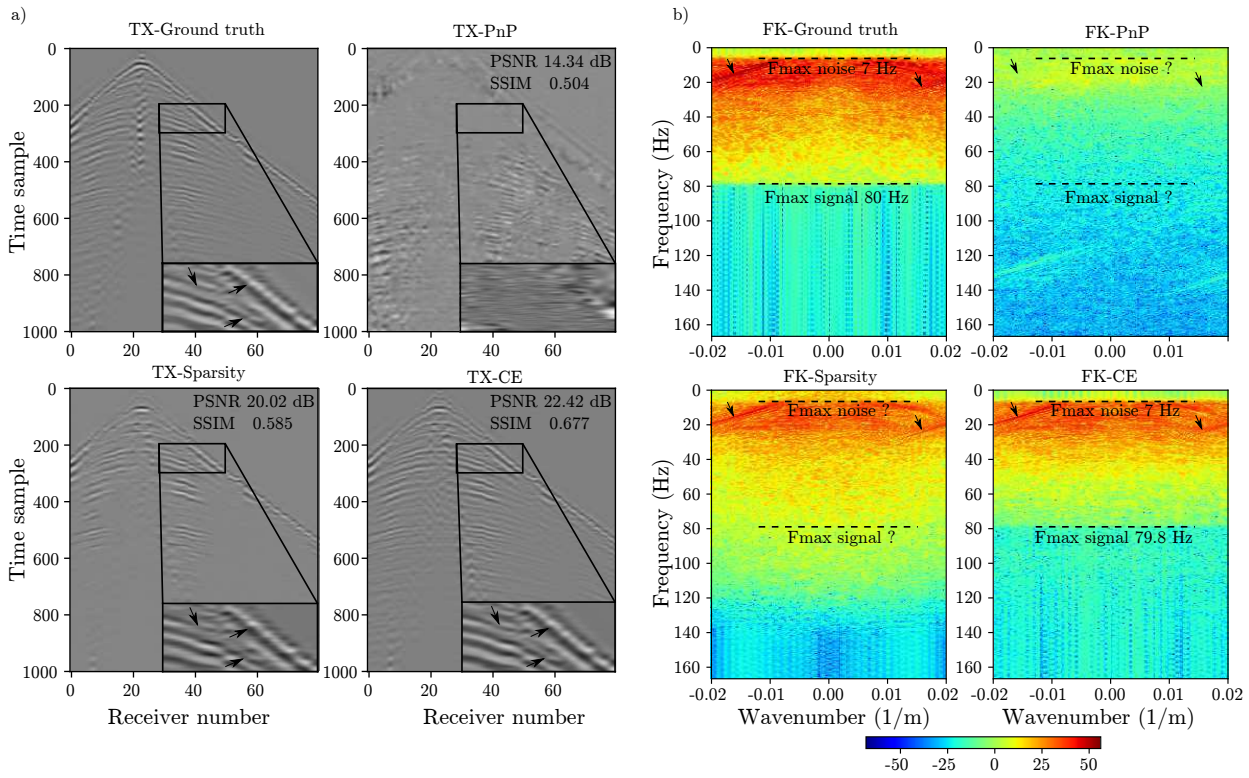

Fig. 3. Reconstruction performance for 20% sampling reduction rate and visual analysis of seismic source 11. a) In time-space domain (TX). (b) In frequency-wavenumber domain (FK).

initialization (i.e. zero initialization) provides the lowest reconstruction quality for all evaluated sampling reduction rates, while the sparsity-initialized PnP (PnP-i) approach provides greatly improved performance, exceeding or equalling that of the sparsity-based method. CE is clearly the best performing method, with significantly better performance than the traditional sparsity-based approach at the 10% and 20%sampling reduction rates. It also has the advantage of not requiring an expensive pre-computed initialization because sparsity prior is directly included with the model.

Table II summarizes the numerical results for each recovered source of one experiment trial using 20% sampling reduction. These results show that the CE substantially improves the quality of seismic events when compared to PnP and Sparsity. Additionally, the proposed scheme is capable of reconstructing both linear structures and reflection hyperbolas, which are a fundamental part of the seismic signals.

TABLE II
COMPARISON OF RECOVERED SOURCE QUALITY METRICS USING 20% SAMPLING REDUCTION RATE FOR PNP, SPARSITY AND CE. THE FINAL ROW INDICATES THE AVERAGE RESULTS ACROSS ALL RECOVERED DATA CUBE.

	PnP		Sparsity		CE	
Source	PSNR (dB)	SSIM	PSNR	SSIM	PSNR	SSIM
2	16.52	0.543	20.83	0.534	**21.21**	**0.591**
7	13.65	0.486	17.49	**0.582**	**18.60**	**0.582**
9	13.39	**0.421**	21.41	0.0.390	**21.75**	0.391
11	14.34	0.504	20.02	0.585	**22.42**	**0.677**
2,7,9,11	15.42	-	19.28	-	**21.94**	-

Figure 3(a) presents the reconstructions of the removed source 11 in time-space (TX) domain for 20% sampling reduction, and their corresponding frequency-wavenumber (FK) representations.The main relevant differences in the seismic signal and reconstructed events are shown with black arrows in the zoomed portions of Fig. 3(a). It can be noted that PnP provides the poorest reconstruction, while all hyperbolic events are well recovered by both Sparsity and CE. However, the Sparsity reconstruction presents some artifacts that mortify the shape of relevant seismic features. On the other hand, the ground truth in Fig. 3(b) shows that the data exhibits a clear frequency range between 7 and 80 Hz. Also, it can be noted that the PnP and Sparsity approaches do not provide clear frequency ranges related to the seismic signal and alias. Meanwhile, CE provides an accurate frequency spectrum with easily noticeable Fmax signal and Fmax noise values at 79.8 Hz and 7 Hz, respectively.

V. CONCLUSION

This work proposes to employ a consensus equilibrium (CE) reconstruction approach to estimate missing seismic sources in cross-spread acquisitions. Unlike traditional reconstruction methods that rely on sparsity priors on universal or learned transformations, CE enables the introduction of various regularization terms in the reconstruction problem, such as the BM3D denoiser along with a sparsity prior, thus, improving the attained source estimations. Simulation results on a real 3D land seismic data set demonstrate the advantages of the proposed method for different sampling reduction rates, with respect to sparsity and plug and play priors. Particularly, CE

provides more accurate results in FK domain, which in turn, avoids error propagation during the seismic data processing workflow, seismic migration and imaging. Quantitatively, CE provides up to 2 dB of PSNR improvement over the traditional sparsity-based approach.

ACKNOWLEDGMENT

This work was supported by the Agreement "Acuerdo No. 27 derivado del Convenio Marco de Cooperación Tecnológica y Científica No. 5222395 UIS–ECOPETROL", and B. Wohlberg by the Laboratory Directed Research and Development program of Los Alamos National Laboratory under project number 20200061DR. The authors thank the Centre for High Performance Computing (GUANE-UIS) for providing computational resources to run the parameter tuning experiments.

REFERENCES

[1] B. Wang and W. Lu, "Accurate and efficient seismic data interpolation in the principal frequency wavenumber domain," *Journal of Geophysics and Engineering*, vol. 14, no. 6, pp. 1475–1483, Dec. 2017.

[2] Y. Wang, "Seismic trace interpolation in the f-x-y domain," *Geophysics*, vol. 67, no. 4, pp. 1232–1239, Jul. 2002.

[3] Y. Liu and S. Fomel, "Trace interpolation beyond aliasing using regularized nonstationary autoregression," in *SEG Technical Program Expanded Abstracts 2010*, vol. 76, no. 5. Society of Exploration Geophysicists, Jan. 2010, pp. 3662–3667.

[4] D. A. B. Oliveira, R. S. Ferreira, R. Silva, and E. Vital Brazil, "Interpolating seismic data with conditional generative adversarial networks," *IEEE Geoscience and Remote Sensing Letters*, vol. 15, no. 12, pp. 1952–1956, 2018.

[5] W. Fang, L. Fu, M. Zhang, and Z. Li, "Seismic data interpolation based on U-net with texture loss," *GEOPHYSICS*, vol. 86, no. 1, pp. V41–V54, Jan. 2021.

[6] D. L. Donoho, "Compressed sensing," *IEEE Transactions on Information Theory*, vol. 52, no. 4, pp. 1289–1306, apr 2006.

[7] E. J. Candès, J. Romberg, and T. Tao, "Robust uncertainty principles: Exact signal reconstruction from highly incomplete frequency information," *IEEE Transactions on Information Theory*, vol. 52, no. 2, pp. 489–509, Feb. 2006.

[8] R. G. Baraniuk and P. Steeghs, "Compressive sensing: A new approach to seismic data acquisition," *The Leading Edge*, vol. 36, no. 8, pp. 642–645, 2017.

[9] T. Jiang, Y. Jiang, D. Clark, and R. Gray, "A compressive seismic field trial and reconstruction test using regular indexing," in *International Exposition and Annual Meeting SEG 2018*. Society of Exploration Geophysicists, 2018, pp. 86–90.

[10] G. Hennenfent, L. Fenelon, and F. J. Herrmann, "Nonequispaced curvelet transform for seismic data reconstruction: A sparsity-promoting approach," *GEOPHYSICS*, vol. 75, no. 6, pp. WB203–WB210, Nov. 2010.

[11] H. Jamali-Rad, B. Kuvshinov, Z. Tang, and X. Campman, "Deterministically Subsampled Acquisition Geometries for Optimal Reconstruction," in *78th EAGE Conference and Exhibition 2016*. EAGE, May 2016, pp. 1–8.

[12] J. Ma and S. Yu, "Sparsity in compressive sensing," *The Leading Edge*, vol. 36, no. 8, pp. 646–652, Aug. 2017.

[13] X. Campman, Z. Tang, H. Jamali-Rad, B. Kuvshinov, M. Danilouchkine, Y. Ji, W. Walk, and D. Smit, "Sparse seismic wavefield sampling," *The Leading Edge*, vol. 36, no. 8, pp. 654–660, 2017.

[14] F. J. Herrmann, M. P. Friedlander, and Ö. Yilmaz, "Fighting the curse of dimensionality: Compressive sensing in exploration seismology," *IEEE Signal Processing Magazine*, vol. 29, no. 3, pp. 88–100, 2012.

[15] Y. Wang, "Sparseness-constrained least-squares inversions: Application to seismic wave reconstruction," *Geophysics*, vol. 68, no. 5, pp. 1633–1638, Sep. 2003.

[16] Q. Liu, L. Fu, and M. Zhang, "Deep-seismic-prior-based reconstruction of seismic data using convolutional neural networks," *GEOPHYSICS*, vol. 86, no. 2, pp. V131–V142, Mar. 2021.

[17] B. Wang, N. Zhang, W. Lu, and J. Wang, "Deep-learning-based seismic data interpolation: A preliminary result," *GEOPHYSICS*, vol. 84, no. 1, pp. V11–V20, Jan. 2019.

[18] H.-M. Sun, R.-S. Jia, X.-L. Zhang, Y.-J. Peng, and X.-M. Lu, "Reconstruction of missing seismic traces based on sparse dictionary learning and the optimization of measurement matrices," *Journal of Petroleum Science and Engineering*, vol. 175, pp. 719–727, 2019.

[19] S. R. Borra, G. J. Reddy, and E. S. Reddy, "Seismic Data Compression using Wave Atom Transform," *Global Journal of Computer Science and Technology: F Graphics and Vision*, vol. 15, no. 1, pp. 35–41, 2015.

[20] F. J. Herrmann and G. Hennenfent, "Non-parametric seismic data recovery with curvelet frames," *Geophysical Journal International*, vol. 173, no. 1, pp. 233–248, Apr. 2008.

[21] M. Leinonen, R. J. Hewett, L. Demanet, X. Zhang, and L. Ying, "High-dimensional wave atoms and compression of seismic data sets," in *Society of Exploration Geophysicists International Exposition and 83rd Annual Meeting, SEG 2013: Expanding Geophysical Frontiers*, vol. 3. Society of Exploration Geophysicists, Sep. 2013, pp. 3591–3596.

[22] J. Liang, J. Ma, and X. Zhang, "Seismic data restoration via data-driven tight frame," *GEOPHYSICS*, vol. 79, no. 3, pp. V65–V74, May 2014.

[23] W. Liu, S. Cao, G. Li, and Y. He, "Reconstruction of seismic data with missing traces based on local random sampling and curvelet transform," *Journal of Applied Geophysics*, vol. 115, no. 115, pp. 129–139, 2015.

[24] P. Yang and S. Fomel, "Seislet-based morphological component analysis using scale-dependent exponential shrinkage," *Journal of Applied Geophysics*, vol. 118, pp. 66–74, Jul. 2015.

[25] O. Villarreal, K. L. López, D. Espinosa, W. Agudelo, and H. A. Fuentes, "Seismic source reconstruction in an orthogonal geometry based on local and non-local information in the time slice domain," *Journal of Applied Geophysics*, p. 103846, sep 2019.

[26] T. Jiang, P. Eick, Y. Jiang, B. Gong, J. Tan, T. Li, K. Koster, D. Enns, and R. Holt, "SEAM phase II Barrett model classic data study: Land compressive seismic acquisition," in *SEG International Exposition and Annual Meeting 2019*. Society of Exploration Geophysicists, 2019, pp. 137–141.

[27] E. J. Candès and D. L. Donoho, "New tight frames of curvelets and optimal representations of objects with piecewise C 2 singularities," *Communications on Pure and Applied Mathematics*, vol. 57, no. 2, pp. 219–266, feb 2004.

[28] S. V. Venkatakrishnan, C. A. Bouman, and B. Wohlberg, "Plug-and-Play priors for model based reconstruction," in *IEEE Global Conference on Signal and Information Processing*, Dec. 2013, pp. 945–948.

[29] G. T. Buzzard, S. H. Chan, S. Sreehari, and C. A. Bouman, "Plug-and-Play Unplugged: Optimization-Free Reconstruction Using Consensus Equilibrium," *SIAM Journal on Imaging Sciences*, vol. 11, no. 3, pp. 2001–2020, Jan. 2018.

[30] Y. Mäkinen, L. Azzari, and A. Foi, "Exact transform-domain noise variance for collaborative filtering of stationary correlated noise," in *2019 IEEE International Conference on Image Processing (ICIP)*, 2019, pp. 185–189.

[31] M. Maggioni, V. Katkovnik, K. Egiazarian, and A. Foi, "Nonlocal transform-domain filter for volumetric data denoising and reconstruction," *IEEE Transactions on Image Processing*, vol. 22, no. 1, pp. 119–133, 2012.

[32] S. Majee, T. Balke, C. A. J. Kemp, G. T. Buzzard, and C. A. Bouman, "4D x-ray CT reconstruction using multi-slice fusion," in *IEEE International Conference on Computational Photography (ICCP)*, 2019.

[33] Y. Mäkinen and L. Azzari and A. Foi, "Python wrapper for BM3D denoising," https://pypi.org/project/bm3d/, 2021, online; accessed 29 January 2021.

[34] R. Shahidi, G. Tang, J. Ma, and F. J. Herrmann, "Application of randomized sampling schemes to curvelet-based sparsity-promoting seismic data recovery," *Geophysical Prospecting*, vol. 61, no. 5, pp. 973–997, Sep. 2013.

[35] B. Hardage and S. Tinker, "Stratton 3D survey," https://dataunderground.org/no/dataset/stratton, 2021, online; accessed 29 January 2021.

[36] Z. Wang, A. C. Bovik, H. R. Sheikh, and E. P. Simoncelli, "Image quality assessment: From error visibility to structural similarity," *IEEE Transactions on Image Processing*, vol. 13, no. 4, pp. 600–612, Apr. 2004.